Inorganic Chemistry

Article

pubs.acs.org/IC

Heptacoordinate Heteroleptic Salan (ONNO) and Thiosalan (OSSO) Titanium(IV) Complexes: Investigation of Stability and Cytotoxicity

Martin Grützke,[†] Tiankun Zhao, Timo A. Immel,[‡] and Thomas Huhn*

Fachbereich Chemie and Konstanz Research School Chemical Biology, Universität Konstanz, Universitätsstr. 10, D-78457 Konstanz, Germany

Supporting Information

ABSTRACT: Seven heptacoordinate titanium(IV) complexes were synthesized based on the concept of hetero-bis-chelate stabilization of salan (ONNO) and thiosalan (OSSO) titanium(IV)alkoxides with 2,6-pyridinedicarboxylic acid (dipic) and derivatives thereof. The resulting compounds were investigated in a solid by X-ray diffraction and in solution by NMR spectroscopy. A thiosalan (OSSO) titanium(IV) complex could be isolated and its conformational stabilization by dipic was shown by ^{1}H NMR spectroscopy to lead to nonfluxional behavior even at room temperature. The stability of selected complexes was assessed at pH 1.9, 6.8, and 12.1 by an UV−vis monitored hydrolysis study with >5 Mio. equivalents of water. Even at pH 12.1 [L^{1}Ti(dipic)^{1}] showed $t_{1/2}$ of more than 2 days. The cytotoxicity of all compounds was investigated in two human carcinoma cell lines. IC_{50}-values in the range of cisplatin were achieved by all tested compounds except for [L^{4}Ti(dipic)^{1}], which was proven to be nontoxic. The functionalization of dipic was thus well tolerated and did neither interfere with the stability nor the cytotoxicity of the heteroleptic complexes.

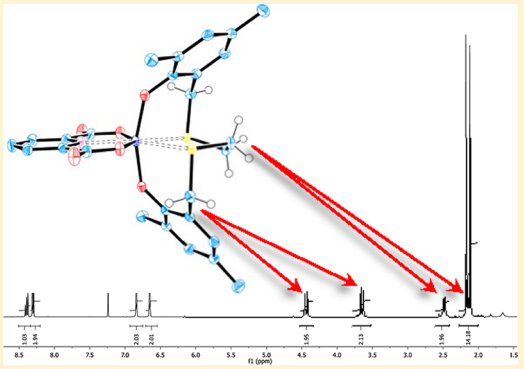

INTRODUCTION

A broad scope of salan complexes (ONNO-binding motif) of late[1,2] and early transition metals[3] has been originally developed as alternatives to metallocenes in diverse fields of organic transformations such as polymerization,[4−6] oxidation,[7] and C−C-bond formation.[8,9] More recently, titanium(IV)-salan alkoxides have been identified and intensely investigated due to their favorable antitumor activity.[10−14] The salan type ligand system offers ample opportunities for chemical modifications influencing steric as well as electronic properties of the resulting titanium complexes. Consequently, this led to the development of complexes bearing differently substituted salan-backbones with certain properties. Halogenation of the phenolate, for example, led to the formation of either strongly cytotoxic titanium-salan alkoxides (fluoro-substitution)[11] or complexes with enhanced stability in aqueous media when chlorine was chosen as the substituent.[15,16] An octahedral Ti(IV)-complex completely lacking any labile ligand showed cytotoxicity after formulation as nanoparticles, most probably because of enhanced cellular uptake.[17] Utilizing chiral amines to bridge both halves of the ligand, however, gave access to chiral complexes showing different cytotoxicities of their respective enantiomers.[18] Recently, the first nontitanium based salan complexes of vanadium(V),[19] ruthenium(III)[20] and copper(II), nickel(II), and zinc(II)[21] were found cytotoxic.

The second half of the coordination sphere of those diverse titanium complexes, the often so-called labile ligand, has been less of a subject of study except for a systematic investigation of the influence on cytotoxicity and stability of several different alkoxides[15] and recently the investigation of differently substituted catechols[22,23] within the same context. Increasing coordinative saturation of a transition metal center by chelating ligands enhances its kinetic inertness against ligand exchange.[24,25]

On the basis of this concept, we recently introduced an exceedingly stable but nevertheless impressively cytotoxic titanium(IV)salan derivative with an enlarged coordination sphere at the central metal.[26] In addition to the dianionic tetradentate salan, an additional dianionic tridentate, namely, pyridine-2,6-dicarboxylic acid was implemented by ligand exchange resulting in exclusive formation of a monomeric heptacoordinate hetero-bis-chelate of pentagonal bipyramidal geometry, which embeds its metal center tightly between both chelators. The resulting complex showed impressive stability in aqueous media at variable pH and was highly active against different cancer cell lines *in vitro* and more importantly in an *in vivo* mouse model of cervical cancer.[13,26]

Here, we describe our results in extending the scope of hetero-bis-chelation toward a broader range of (i) different salan complexes with (ii) different substituted pyridine-2,6-dicarboxylates. The stability and cytotoxicity of the resulting hetero-bis-chelates are reported. We were especially interested in the influence of different substitution patterns at both

Received: December 2, 2014
Published: July 7, 2015

DOI: 10.1021/acs.inorgchem.5b00690
Inorg. Chem. 2015, 54, 6697−6706

Scheme 1. Metalation of Salan Ligands H_2L^{1-6} by Titanium Tetraisopropoxide and Further Modification of the Ligand-Sphere by Exchange of Isopropoxide against Substituted Dipicolinates (Dipic)$^{1-3}$

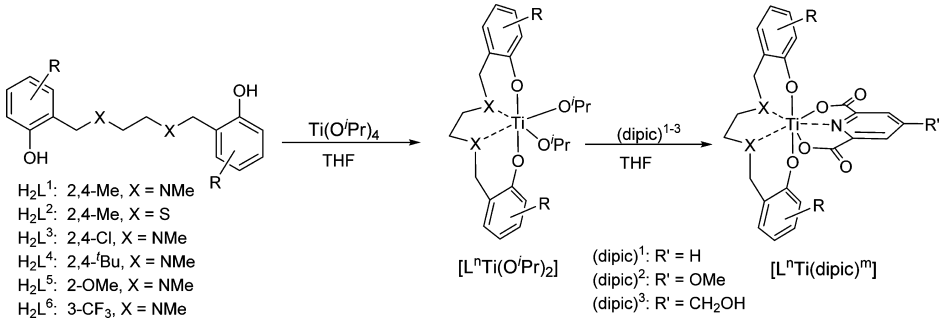

chelators on structure, stability, and activity in cytotoxicity assays in view of further modifications.

RESULTS AND DISCUSSION

Complex Synthesis. Preparation of the salan ligands H_2L^{1-6} followed established procedures starting from substituted salicylic aldehydes,[27,28] substituted phenols,[29] or in the case of the thiosalan from 2-(bromomethyl)-4,6-dimethylphenol.[30,31] Metalation of these diaryl-salan ligands H_2L^{1-6} with titanium tetraisopropoxide in tetrahydrofuran resulted in clean and fast formation of the metalation products $[L^{1-6}Ti(O^iPr)_2]$ as racemic mixtures. The reaction progress was followed by NMR spectroscopy, and metalation was usually completed within 12 h. The bis-alkoxides were then either isolated or used in the next step without purification (Scheme 1). Metalation of H_2L^2 proceeded markedly faster and had finished after 3 h. Longer reaction times resulted in diminished yields because decomposition sets in progressively (*vide infra*).

To these yellow solutions of $[L^{1-6}Ti(O^iPr)_2]$ in THF were then added pyridine-2,6-dicarboxylic acid (H_2dipic^1), 4-methoxypyridine-2,6-dicarboxylic acid (H_2dipic^2),[32] or 4-(hydroxymethyl)pyridine-2,6-dicarboxylic acid (H_2dipic^3) (Scheme 1).[33,34] The initially heterogeneous reaction mixtures gradually got homogeneous over time, and the color turned from a faint yellow toward a dark red when all isopropoxide was finally exchanged. The exchange was controlled by TLC and by measuring ^{1}H NMR spectra of reaction samples after the complete removal of solvent. The reaction was considered to be complete when no resonances from Ti-bound isopropoxo-ligands were detectable.

Complexes $[L^2Ti(dipic)^1]$, $[L^3Ti(dipic)^1]$, and $[L^1Ti(dipic)^3]$ precipitated from the reaction mixture upon partial solvent removal and could be isolated in analytically pure state after filtration, washing with small amounts of solvent and thoroughly drying under reduced pressure. All other complexes (entries 1 and 4–7, Table 1) have been isolated by flash column chromatography on ordinary silica gel using standard conditions, namely, stock solvents and without special exclusion of oxygen or humidity. Interestingly, after solvent removal at the rotary evaporator trace amounts of solvent were impossible to remove as was evident in ^{1}H NMR spectra. Lowering the pressure to 10^{-3} mbar had no positive effect. Finally, we heated a sample to 170 °C for 24 h at 10^{-3} mbar and positively noted that we (i) removed all solvent traces and (ii) that the complexes were not damaged as was evident from proton NMR spectra. This procedure worked equally well for all complexes in Table 1 except for $[L^2Ti(dipic)^1]$, which already lost all solvent traces upon evacuation to 10^{-3} mbar at room temperature (r.t.).

Table 1. Selected ^{1}H NMR Chemical Shift-Values of Hetero-bis-chelates with Dipic$^{1-3}$ as a Second Chelator (Entries 2–4, 6, and 8) in Comparison to Their Parent Isopropoxo-Complexes (Entries 1, 5, and 7)[a]

entry		NCH_2CH_2N [ppm]		$Ar-CH_2$ [ppm]		Ar–CH [ppm]	
1	$[L^1Ti(O^iPr)_2]$	1.73	3.03	3.06	4.69	6.61	6.89
2	$[L^1Ti(dipic)^1]$	2.11	3.36	3.13	5.27	6.63	6.74
3	$[L^1Ti(dipic)^2]$	2.10	3.35	3.12	5.25	6.63	6.75
4	$[L^1Ti(dipic)^3]$	2.10	3.34	3.13	5.25	6.63	6.71
5	$[L^3Ti(O^iPr)_2]$	1.88	2.91	3.14	4.63	6.86	7.28
6	$[L^3Ti(dipic)^1]$	2.26	3.29	3.21	5.34	6.91	7.16
7	$[L^4Ti(O^iPr)_2]$	1.83	3.18	3.12	4.42	6.76	7.20
8	$[L^4Ti(dipic)^1]$	2.29	3.56	3.24	5.26	6.84	7.08

[a] ^{1}H NMR are measured in $CDCl_3$.

Structure Discussion (NMR/X-ray). The alkoxo-complexes of the diarylamino-substituted salan ligands show the typical AB pattern of the diastereotopic $Ar-CH_2-N$-protons in their ^{1}H NMR spectra. This is characteristic for the *fac-fac* coordination of the salan in an octahedral complex with C_2 symmetry.[15,35] In the ^{1}H NMR of the diarylthio-substituted salan $[L^2Ti(O^iPr)_2]$, these benzylic protons are represented by a singlet indicating their magnetic equivalence. A diminished conformational stability of the homologue *tert*-butyl titanium(IV)thiosalan bis-isopropoxide has been previously reported by Kol and co-workers.[31] Utilizing variable-temperature NMR experiments, they have demonstrated that the complex adopts a fluxional behavior at r.t., whereas at lower temperature the benzylic protons of the $Ar-CH_2-S$-groups showed the expected AB-pattern of a C_2-symmetric complex. The attempted isolation of $[L^2Ti(O^iPr)_2]$ was unsuccessful and resulted in the formation of oligomeric material of unknown composition. Instead, $[L^2Ti(O^iPr)_2]$ was subjected to *in situ* ligand exchange with dipic^1.

All hetero-bis-chelates $[L^{1-6}Ti(dipic)^{1-3}]$ were characterized in solution by ^{1}H NMR spectra as forming single geometric isomers with structural features very similar to their parent alkoxides with the notable difference of strongly downfield shifted resonances of all of the diastereotopic $N-CH_2-CH_2-N$ protons of the backbone in the order of ~0.4 ppm (Table 1). While one of the two diastereotopic benzylic $Ar-CH_2$ protons is shifted by only around 0.1 ppm downfield, the second proton experiences a strongly enhanced downfield shift. The difference in magnitude of the shift is dependent on the nature of the salan substituent. For the bulkiest $[L^4Ti(dipic)^1]$, the resonance

DOI: 10.1021/acs.inorgchem.5b00690
Inorg. Chem. 2015, 54, 6697–6706

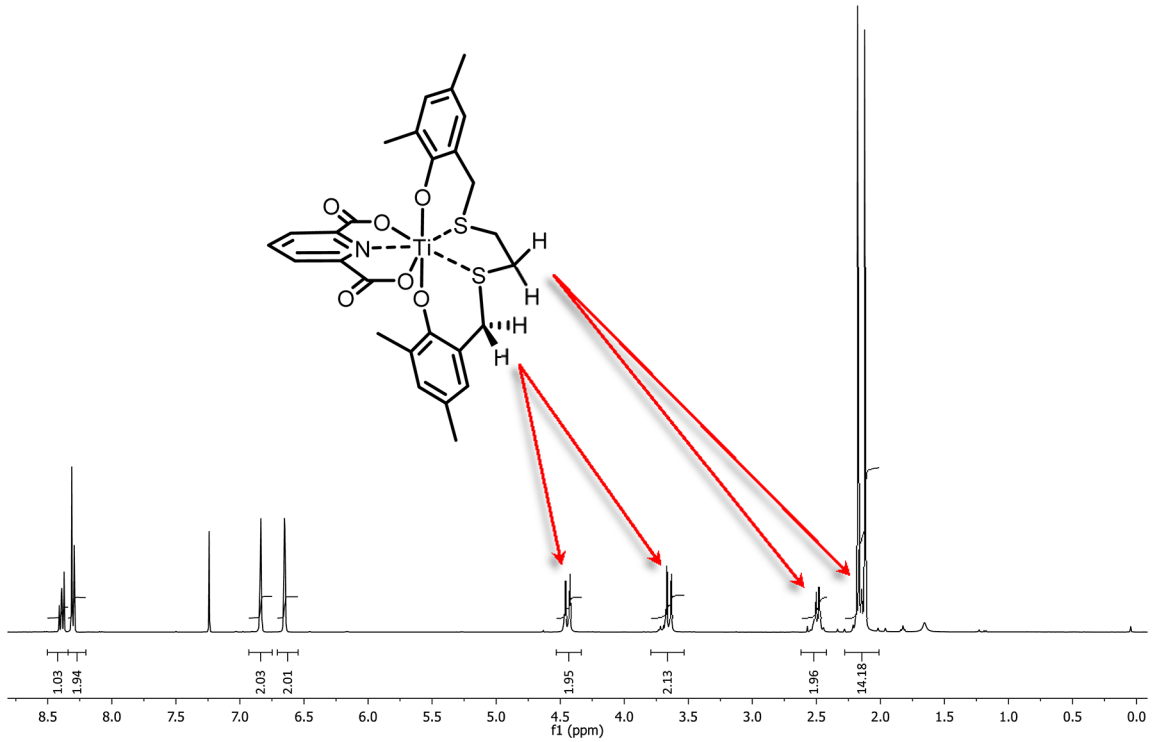

Figure 1. ^{1}H NMR spectrum ($CDCl_3$) of [L^2Ti(dipic)^1] at r.t. Upon exchange of both isopropoxo-ligands with pyridine-2,6-dicarboxylate, protons of the bridging thioether become diastereomeric in solution even at r.t. due to enhanced conformational rigidity enforced by the second chelating ligand.

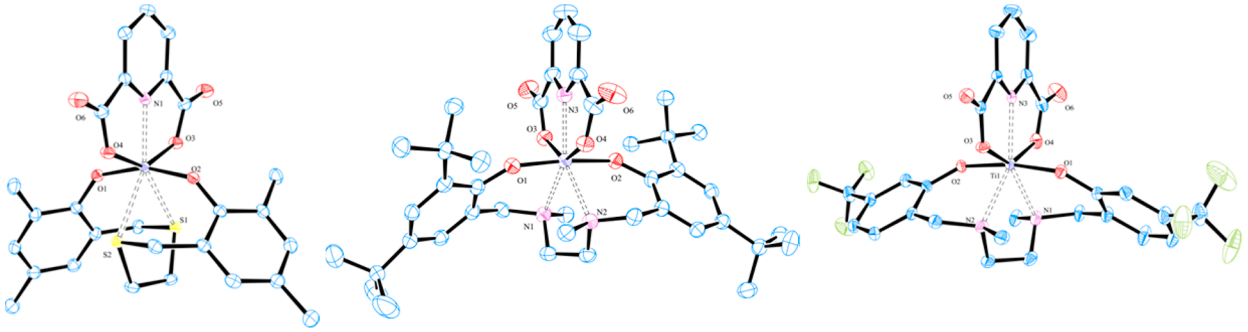

Figure 2. ORTEP diagram of [L^2Ti(dipic)^1] (left), [L^4Ti(dipic)^1] (middle), and [L^6Ti(dipic)^1] (right). Thermal ellipsoids are drawn at the 50% probability level. Hydrogen atoms and solvent molecules are omitted for clarity. Single crystals suitable for X-ray diffraction were either grown by slow diffusion of hexane in saturated solutions of [L^4Ti(dipic)^1] and [L^6Ti(dipic)^1] in DCM or by slow evaporation of a saturated solution of [L^2Ti(dipic)^1] in $CHCl_3$.

is shifted by more than 0.8 ppm downfield, and we reason that this proton is forced closer into the direction of the anisotropy cone of the salans phenolate. The magnitude of the chemical shift is apparently independent from the nature of the dipic-derivative (cf. Table 1, entry 1 vs entries 2−4).

The characteristic AB-pattern of the benzylic Ar−CH_2 protons is indicating the conservation of the *fac-fac* (*cis-α*) binding mode of the salan ligand thus being consistent with C_2-symmetry in solution. This is most prominently demonstrated in the spectrum of [L^2Ti(dipic)^1] with the additional chelator enhancing the complex's rigidity (Figure 1). Even at r.t., the spectrum shows no evidence of fluxional behavior; instead, the characteristic AB-pattern of a rigid and highly symmetric complex becomes apparent. Compared to its parent alkoxide, thiosalan [L^2Ti(dipic)^1] is stable in solution and can be isolated in crystalline form and stored without restriction.

The NMR based structure assignment in solution is confirmed in the solid by X-ray diffraction of three representative examples. The dark red thiosalan [L^2Ti(dipic)^1] crystallizes in the triclinic space group *P*-1 with an additional molecule of chloroform in the asymmetric unit. The complex adopts the geometry of a distorted pentagonal-bipyramid with the sulfur atoms S1 and S2, the pyridine nitrogen, and the carboxylate oxygen atoms O3 and O4 forming the equatorial plane of the pentagon and the phenolates O1 and O2 in the apical position (Figure 2). A similar structure is adopted by [L^4Ti(dipic)^1] and [L^6Ti(dipic)^1]. While [L^4Ti(dipic)^1] crystallizes in the orthorhombic space group *Pbca* without additional solvent molecules, [L^6Ti(dipic)^1] crystallizes in the triclinic space group *P*-1 with half a molecule of *n*-hexane in the asymmetric unit. The hexane is located at a center of inversion, and its terminal CH_3-group was found to be strongly disordered. A suitable model was not found; instead, the

DOI: 10.1021/acs.inorgchem.5b00690
Inorg. Chem. 2015, 54, 6697−6706

hexane was refined isotropically without added hydrogen atoms. This accounts for the high value of remaining electron density (2.25 eÅ^{-3}) close to C52 and C51 of the solvent molecule.

A detailed structure search in the CSD database revealed only a very limited number of salan based titanium complexes with an additional chelating ligand (details see Supporting Information, Table S9). From a total of 8 complexes, five are utilizing substituted catechols[23] or catechol itself[22] as a second chelator, leading to favorable 5-ring chelates, two using ω-hydroxycarboxylic acids,[35] forming either 5- or 6-ring chelates, and one being the dipic derivative [L^{1}Ti(dipic)^1].[26] In all these previously reported complexes, the salan is showing *cis-β* geometry with the two phenolato ligands in *cis* disposition resulting in C_1 symmetry except in [L^{1}Ti(dipic)^1] where the salan geometry is *cis-α* in the solid and in solution. The 2,6-pyridyldicarboxylates bite-angle of around 140° paired with the ability to form two five-ring chelates simultaneously results in the preferable formation of the C_2-symmetric *cis-α* isomer. Hence, [L^{1}Ti(dipic)^1] and all other reported dipic-modified complexes here have their salan phenoxides oriented *trans*, while both amino groups are oriented *cis*. The dipicolinates thus resemble in this respect the structure of their parent titanium bis-isopropoxides.

The steric demand and the softer nature of the sulfur atoms in [L^{2}Ti(dipic)^1] weakens the Ti−S bonds and forces the titanium slightly outward in direction toward the pyridine-2,6-dicarboxylate. With an average of 2.676 (1) Å, the Ti−S bond is considerably shorter than that in similar titanium thiosalan isopropoxides where the Ti−S bond assumes values of 2.70−2.73 Å[36−38] because of the less electron rich nature of the dipicolinate compared to the higher donor strength of the alkoxides. Whereas in [L^{4}Ti(dipic)^1] and [L^{6}Ti(dipic)^1] the O1−Ti−O2 axis adopts an almost linear style with angles of 174.44(10)° and 170.62(9)°, respectively, the axis in [L^{2}Ti-(dipic)^1] has a distinct kink and assumes a value of only 161.33(8)° (Table 2). This effect is compensated by a wider bite angle of the two carboxylic groups of the dipic with angles for O3−Ti−O4 of 144.72(7)° in the case of the thiosalan compared with 142.23(9)° and 141.93(8)° for [L^{4}Ti(dipic)^1] and [L^{6}Ti(dipic)^1], respectively. As a consequence, the pyridine-2,6-dicarboxylate's N3−Ti distance becomes significantly shorter in [L^{2}Ti(dipc)^1] (2.148(2) Å) compared to that in [L^{4}Ti(dipic)^1] and [L^{6}Ti(dipic)^1] (2.185(3) Å). In contrast, the phenolate-Ti distance in [L^{2}Ti(dipic)^1] (avg. 1.850(2) Å) and [L^{4}Ti(dipic)^1] (avg. 1.848(2) Å) is surprisingly unaffected by the substitution pattern of the salan (for a complete set of tabulated structure information, see Supporting Information). The recently characterized [L^{1}Ti(dipic)^1] showed with 1.847(2) Å (average) a comparable O1, O2−Ti distance.[26] In contrast to the *cis-α* configured titanium-salan dipicolinates, *cis-β* configured complexes with ω-hydroxycarboxylic acids or catechol show a greater dissimilarity in the two Ti−phenoxide distances spanning a wider range from 1.84 up to 1.89 Å.[22,23,35] This effect is mainly based on the two different *trans*-oriented partners resulting from the lower symmetry of these complexes. However, in [L^{6}Ti(dipic)^1] the negative inductive effect of the CF_3 group has a noticeable impact on the aryloxide-titanium bond length. With an average of 1.862(2) Å, it is considerably longer than that in the other members of this complex family. This loss of stabilization is compensated by a significantly shortened Ti-carboxylate distance (O3, O4−Ti; avg. 2.033(2) Å) compared to that of [L^{4}Ti(dipic)^1] (avg. 2.057(2) Å), [L^{2}Ti(dipic)^1] (avg. 2.049(2) Å), and [L^{1}Ti(dipic)^1] (avg. 2.049(2) Å).[26] All four members of this family adopt very similar structural features. In the case of [L^{2}Ti(dipic)^1], they are governed by the soft nature and the steric bulk of the thioether bridge, while in [L^{6}Ti(dipic)^1] the electronic effect of the CF_3-group is the dominating feature.

Table 2. Selected Bond Lengths (Å) and Angles (Deg) for Complexes [L^{2}Ti(dipic)^1], [L^{4}Ti(dipic)^1], and [L^{6}Ti(dipic)^1] As Determined by X-ray Diffraction

	[L^{2}Ti(dipic)^1]	[L^{4}Ti(dipic)^1]	[L^{6}Ti(dipic)^1]
N1−Ti	2.662(1)[a]	2.380(3)	2.341(3)
N2−Ti	2.691(1)[b]	2.377(3)	2.379(3)
O1−Ti	1.857(2)	1.854(2)	1.862(2)
O2−Ti	1.843(2)	1.841(2)	1.861(2)
N3−Ti	2.148(2)[c]	2.185(3)	2.185(2)
O3−Ti	2.042(2)	2.063(2)	2.033(2)
O4−Ti	2.056(2)	2.051(2)	2.033(2)
O1−Ti−O2	161.33(8)	174.44(10)	170.62(9)
N1−Ti−N2	74.51(2)[d]	72.72(9)	73.55(9)
O3−Ti−O4	144.72(7)	142.23(9)	141.93(8)

[a]S1−Ti. [b]S2−Ti. [c]N1−Ti. [d]S1−Ti−S2.

Stability and Hydrolysis. In a former NMR-based hydrolysis study, we showed [L^{1}Ti(dipic)^1] to be stable over the course of several weeks in a [D8]-THF/D_2O mixture with no detectable decomposition.[26] For reasons of solubility and accompanied detection limits of NMR, the water content is limited to around 1000 molar equiv. The aqueous chemistry of Ti(IV) species at different pH was recently comprehensively reviewed.[39] At low pH, protons compete with Ti(IV) for ligand binding; at higher pH, the hydroxide competes with the ligands for Ti(IV) binding, and it is well accepted that the pH plays a crucial role in the kinetics of the hydrolysis and the type of products formed.[39] Keeping in mind that heptacoordinate Ti(IV) complexes have added kinetic stability, we wanted to investigate how these complexes might react on exposure to even larger amounts of water and more importantly how the pH-value of the medium influences their stability. Therefore, the hydrolysis of selected complexes was now investigated by time-resolved UV−vis spectroscopy by following the gradual decay of the ligand-to-metal charge transfer band (LMCT) absorbance upon the addition of a large excess of ∼5.0 Mio. molar equiv of a buffer-solution of a given pH to a dilute solution of complex in THF. The LMCT band in dipic-salan complexes has an absorption at around 400 nm and is red-shifted by around 70 nm compared to that of its parent alkoxides (Figure S13, Supporting Information, gives a side by side comparison of UV−vis spectra of [L^{1}Ti(O^{i}Pr)$_2$] and [L^{1}Ti(dipic)^1] recorded in THF). This electronic effect of the dipic-ligand enables us to follow the loss of either the salan or the dipic ligand during hydrolysis. Half-lives of complexes were calculated based on the decrease of their LMCT band and are summarized in Table 3. Decomposition followed a pseudo-first-order reaction rate in all cases (Figure 3). Throughout the text, the pH of the pure buffer will be used and denoted as pH* when admixed with THF (see Experimental Section for a discussion of the influence of added THF on the pH of an aqueous buffer). Briefly, complexes [L^{1}Ti(dipic)^1], [L^{2}Ti-(dipic)^1], and [L^{4}Ti(dipic)^1] were dissolved in THF and diluted until the UV−vis absorption reached 0.5 (∼1 × 10^{-5} M). These solutions were then mixed with equal volumes of the

DOI: 10.1021/acs.inorgchem.5b00690
Inorg. Chem. 2015, 54, 6697−6706

Table 3. Half-Lives of [L¹Ti(dipic)¹], [L²Ti(dipic)¹], and [L⁴Ti(dipic)¹] at Different pH*-Values Determined in 50:50 (v/v) THF/Phosphate Buffer at 37 °C

	$t_{1/2}$ [h] at		
complexes	pH* 1.9	pH* 6.8	pH* 12.1
[L¹Ti(dipic)¹]	140	150	50
[L²Ti(dipic)¹]	<1 s	<1 s	<1 s
[L⁴Ti(dipic)¹]	stable[a]	stable[a]	stable[a]

[a]No decomposition after 6 days.

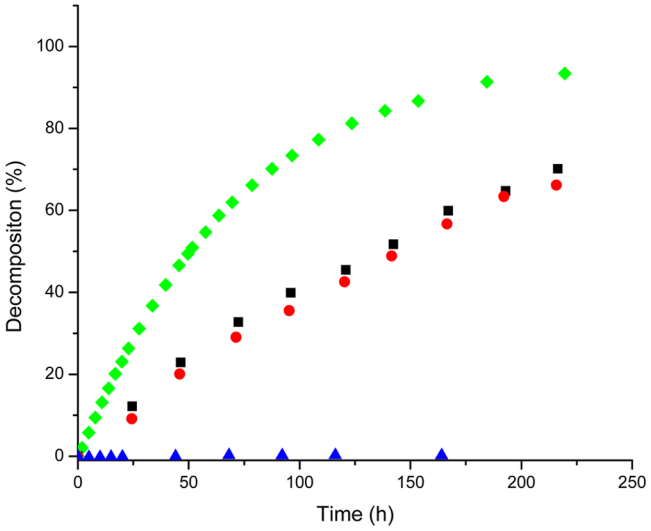

Figure 3. Hydrolysis of [L¹Ti(dipic)¹] in aqueous phosphate buffer/THF (50:50, *v/v*) at three different pH-values (black squares: pH* 1.9; red dots: pH* 6.8; green diamonds: pH* 12.1) and [L⁴Ti(dipic)¹] at pH* 12.1 (blue triangles), data at pH* 1.9 and 6.8 are not shown. Decomposition followed by UV−vis spectroscopy.

particular phosphate buffer of either pH 1.9, 6.8, or 12.1 to afford a 50:50 mixture, and initial spectra were recorded immediately afterward (t = 0). Measurements were repeated in frequent time intervals; in between, samples were stored at 37 °C (see Figure S14−S16, Supporting Information, for time-resolved spectra).

During the measurement of [L¹Ti(dipic)¹], a slow decrease of UV-absorption over time becomes apparent at all three pH-values. A closer inspection of the different spectra recorded during more than 200 h reveals that at any given pH all absorption bands are decreasing simultaneously without any noticeable shift toward a different wavelength which might have pointed to the formation of a (transient) intermediate.[22,40] The stability at lowest and neutral pH is with a half-life of around 6 days remarkably high for a titanium(IV) species and exceeds our standard incubation time more than 3-fold. At pH* 12.1, [L¹Ti(dipic)¹] is decomposing slightly faster, but with a half-life of 50 h it is still highly resistant. Compared to the NMR-based study with a limited amount of added water, the conditions used here for the hydrolysis of [L¹Ti(dipic)¹] with a buffered pH* of 6.8 and a large excess of >5 Mio. equiv. water are of more biological relevance. At the end of the observation time of 9 days, only the sample at highest pH lost all absorbance in the visible region (Figure S16, Supporting Information), while in the two other cases, some starting material is still detectable. After prolonged incubation times, all spectra showed remaining absorption at 270−300 nm only which can be attributed to mixtures of salan and dipic ligands (cf. Figure S12, Supporting Information). In parallel experiments, solutions of [L¹Ti(dipic)¹] in THF were reacted with variable amounts of water. In contrast to hydrolysis experiments done with salan-alkoxides where a trinuclear μ-oxo bridged complex could recently be isolated,[22] after prolonged time we isolated either unreacted starting material or observed a slow liberation of ligands. No other products could be observed. This can be rationalized by steric effects of dipic compared to monodentate alkoxo ligands or by assuming an interchange mechanism where upon the attack of water (or OH^- from autoprotolysis) on the complex one bond to either the salan or the dipic is weakened or might get broken with the incoming nucleophile occupying the now vacant coordination site. Since both salan and dipic are multidentates, the back reaction is favored because the chelator remains partly bound and stays within close proximity to the titanium.[24] When the partly dissociated multidentate becomes efficiently solvated, thus facilitating its stepwise exchange and preventing it from rebinding, the dissociation might lead ultimately to a breakdown of the complex's integrity. Under these conditions, a large excess of solvent, i.e., high dilution, excess of nucleophile, the formation of μ-oxo bridged species is less likely because a second molecule of partially hydrolyzed complex in close vicinity is needed. Instead, in an alternative scenario the transient hydroxo titanium species is likely to be further attacked by excess solvent and/or nucleophile to end up finally as titanium-oxo species with liberation of the ligands, as was observed during our long-term UV-experiments.

In contrast to [L¹Ti(dipic)¹], [L⁴Ti(dipic)¹] did not show any decrease in intensity of the LMCT-band during the observation period of 6 days at all three pH-values (Figure 3 and Table 3). Obviously, the bulky *tert.*-butyl groups in conjunction with a second chelating agent present an efficient kinetic barrier against either nucleophilic attack at the Ti(IV) center at high pH or protonation of the ligand system at low pH. During previous NMR-based hydrolysis studies of the parent alkoxide [L⁴Ti(O^{i}Pr)$_2$], its half-life in added D_2O was determined between 2−10 h at 37 °C.[15,22] Under these conditions, liberation of the salan ligand was observed. Seemingly, the *tert*-butyl groups alone do not suffice to enforce kinetic stability to the hard-Ti(IV) center and only after the substitution of both alkoxides by the tridentate dipic and formation of the hetero-bis-chelate [L⁴Ti(dipic)¹] an efficient kinetic stabilization even under basic conditions is achieved. For the thiosalan [L²Ti(dipic)¹], the concept of stabilization by dipic showed its limitations. While [L²Ti(dipic)¹] is efficiently stabilized by dipic in nonaqueous media as evident from the NMR spectra and in the solid (*vide supra*), the deeply red colored solution of [L²Ti(dipic)¹] in THF decolorized immediately at each tested pH upon contact with the buffer medium. Thus, the half-life could not be exactly determined by UV−vis spectroscopy and was estimated to be below 1 s. This lack of stability can be rationalized in terms of different donor strength of the N−Me group compared with the sulfur-atoms of the thiosalan and by steric means. While the *N*-methyl group is a quite hard donor and efficiently stabilizes the likewise hard Ti(IV)-center,[41] the thiosalan is considered a soft donor, and stabilization becomes less effective.[31,37]The bigger covalent radius of sulfur increases the Ti−S distance to ∼2.7 Å, compared with ∼2.4 Å for the salan complex (Table 2), resulting in a flexible and hence more vulnerable backbone.[42] ^{1}H NMR spectra of [L²Ti(dipic)¹] recorded in D_2O/THF mixtures revealed the fast liberation of the ligand system.

DOI: 10.1021/acs.inorgchem.5b00690
Inorg. Chem. 2015, 54, 6697−6706

Cytotoxicity Assay. Except for $[L^2Ti(dipic^1)]$, all salan complexes were tested in an AlamarBlue assay for their cytotoxic behavior against HeLa S3 and Hep G2 human cancer cells. All complexes $[L^{1,3-6}Ti(dipic)^1]$ bearing unmodified dipic as well as complexes $[L^1Ti(dipic)^{2-3}]$ with substituted 2,6-pyridinedicarboxylic acid with the exception of $[L^4Ti(dipic)^1]$ showed strong cytotoxicity in the low micromolar regime against both cell lines used (the results are summarized in Table 4). $[L^3Ti(dipic)^1]$ and $[L^6Ti(dipic)^1]$ (entries 2 and 5, Table 4) are the complexes with the highest cytotoxicity against both cell lines. With an up to 3-fold enhanced activity, they outperform the other members of this panel and are even more active than their parent isopropoxide.[11,43] With inhibitory values in the region of 1.3−2.4 μM, their activity compares very well with that of cisplatin (entry 8). The slightly less cytotoxic complexes $[L^1Ti(dipic)^1]$, $[L^1Ti(dipic)^2]$, and $[L^1Ti(dipic)^3]$ feature the same core complex but have a different substitution pattern at the dipic ligand. The added methoxy- and hydroxymethyl-group at the 4-position of the 2,6-dipicolinic acid enhanced the solubility of $[L^1Ti(dipic)^2]$ and $[L^1Ti(dipic)^3]$ in aqueous media but had virtually no influence on the bioactivity (Table 4, entries 1, 6, and 7). All three complexes show a very balanced activity against both tested cell lines. H_2dipic^1 and its two derivatives $H_2dipic^{2,3}$ were tested to be nontoxic (Figure S3, Supporting Information).

Table 4. Variation of Ligand System−Influence on Cytotoxicity after 48 h of Incubation with Complexes

		IC_{50} [μM][a]	
entry	complex	HeLa S3	Hep G2
1	$[L^1Ti(dipic)^1]$[26]	4.5 ± 0.5	3.2 ± 0.6
2	$[L^3Ti(dipic)^1]$	1.5 ± 0.5	1.6 ± 0.5
3	$[L^4Ti(dipic)^1]$	nontoxic	nontoxic
4	$[L^5Ti(dipic)^1]$	5.1 ± 0.5	4.7 ± 0.1
5	$[L^6Ti(dipic)^1]$	1.3 ± 0.3	2.4 ± 1.6
6	$[L^1Ti(dipic)^2]$	3.4 ± 0.2	4.9 ± 1.1
7	$[L^1Ti(dipic)^3]$	3.6 ± 0.9	2.8 ± 1.0
8	cisplatin[b]	1.2 ± 0.4	3.0 ± 1.3

[a]Maximum inhibition in all cases is >95% except for $[L^4Ti(dipic)^1]$. [b]Cisplatin was used as a reference.

The bulky di-*tert*-butyl-substituted complex $[L^4Ti(dipic)^1]$ was found nontoxic in both cell lines. Its parent alkoxo complex $[L^4Ti(O^iPr)_2]$ has recently been tested to be nontoxic in several cell lines like HT-29,[22,44] OVCAR-1,[22] MCF-7, L-929,[44] Hela S3, and Hep G2.[15] Intracellular accumulation studies in HT-29 cells showed that this lack of bioactivity is not based on limited cellular uptake. After 24 h of incubation, the intracellular titanium concentration was on par with that of the cytotoxic Ti(IV)salan complexes.[44] In contrast to a structurally similar titanium bis-alkoxide based on a tripodal diamine bis-phenolate[3] which formes μ-oxo-bridged dimeric structures of moderate cytotoxicity,[40] neither $[L^4Ti(O^iPr)_2]$ nor $[L^4Ti(dipic)^1]$ forms μ-oxo bridged species during hydrolysis, albeit for different reasons. Whereas the former releases its salan ligand upon hydrolysis already in the presence of 1000 equiv of water[15,22] the latter does not hydrolyze even at pH 12 and >5 Mio. equiv water. Apparently, steric hindrance by the *tert*-butyl groups prevent the formation of multinuclear species for $[L^4Ti(O^iPr)_2]$, while in $[L^4Ti(dipic)^1]$ the second chelator efficiently prevents hydrolysis and renders the complex kinetically inert.

If the complex has labile, i.e., nonchelating ligands and steric reasons permit, the formation of species like the trinuclear μ-oxo bridged compound $[(L)^3Ti_3(\mu_2\text{-}O)_3]$ which showed limited toxicity in HT-29 cells[44] but was highly toxic when formulated as nanoparticles becomes likely.[17] For titanium-(IV)bis-alkoxides with a longer (but not indefinite) half-life, multi nuclear oxo bridged species might form after internalization of the unhydrolysed precursor complex. In this context, recent investigations identified the mitochondria as one possible intracellular target.[45] These diamine bis-phenolate-bound titanium(IV) alkoxides hydrolyze in the course of hours to days in NMR experiments with their limited amount of water.[15,22]

This now arouses the question, why do other "stable" complexes show appreciable bioactivity whereas $[L^4Ti(dipic)^1]$ does not? In $[L^4Ti(dipic)^1]$, the titanium(IV) center is closely surrounded by the dipic and the bulky *tert*- butyl substituted salan (c.f. Figure 2, middle) making the whole complex kinetically inert even when a very large excess of water at pH 12 is employed. The stability of other complexes has been assessed by NMR experiments with ∼1000 equiv of D_2O. While this testing method has been extremely helpful in identifying intermediates, it is technically limited in the amount of added water.[46] In short, while its stability renders $[L^4Ti(dipic)^1]$ kinetically inert, other titanium(IV)salan complexes are only kinetically stabilized but not inert, i.e., they do hydrolyze slowly as is the case with the methyl substituted $[L^1Ti(dipic)^1]$ which is stable for weeks in the NMR study[26] but hydrolyzes with a $t_{1/2}$ of more than 6 days at neutral pH in the UV experiment. Complexes like the recently reported tetrakis phenolate complex[17] or heptacoordinate complexes like $[L^1Ti(dipic)^1]$[26] do not form multinuclear species. The absence of any detectable intermediate during the hydrolysis of $[L^1Ti(dipic)^1]$ has its reason most probably in the second chelator dipic which suppresses the formation of oxo-bridged species. While heptacoordinate $[L^1Ti(dipic)^1]$ is highly cytotoxic as is, the *tetrakis*-phenolato complex was tested to be toxic only when nanoencapsulated probably to facilitate cellular uptake.[17] We conclude from these data that heptacoordinate complexes of the type [LTi(dipic)] can be readily internalized as is by Hela S3 and Hep G2 cancer cells.

CONCLUSIONS

In conclusion, we have shown that salan complexes of titanium can be stabilized by 2,6-dipicolinic acid and its derivatives. The resulting heptacoordinate complexes have added kinetic stability over their parent bis-alkoxo complexes and are highly resistant to hydrolysis over a broad pH-range. The concept of hetero-bis-chelation leads to C_2 symmetric Ti(IV) systems which are structurally well-defined, and the resulting complexes are highly bioactive and do not rely on labile ligands and are cytotoxic without the need for special formulation schemes. Their synthesis is straightforward and high yielding, and complexes can be isolated by column chromatography under ambient conditions. More importantly, modifications of the dipicolinic acid by polar groups like methoxy or hydroxymethyl have no negative influence on cytotoxicity and open up possibilities for further derivatization. The resulting complexes were tested highly cytotoxic in two human carcinoma cell lines and show inhibitory values comparable to or better than that of the parent complex $[L^1Ti(dipic)^1]$.

DOI: 10.1021/acs.inorgchem.5b00690
Inorg. Chem. 2015, 54, 6697−6706

EXPERIMENTAL SECTION

The following starting materials were prepared according to known procedures: 4-methoxypyridine-2,6-dicarboxylic acid (H_2dipic^2),[32] 4-(hydroxymethyl)pyridine-2,6-dicarboxylic acid (H_2dipic^3),[33,34] salans $H_2L^{1,4,6}$,[27] H_2L^2,[30,31] H_2L^3,[4] and H_2L^5.[28] Titanium(IV) tetraisopropoxide (99%) and pyridine-2,6-dicarboxylic acid (dipic^1) were purchased from ABCR, and all other chemicals and solvents were purchased from commercial suppliers and purified or dried when necessary.[47] Until otherwise noted, all reactions were carried out without special exclusion of atmosphere. Silica gel 60 (40−63 μm) for flash chromatography was purchased from Macherey & Nagel (Düren). ^{1}H NMR (400 MHz) and ^{13}C NMR (101 MHz) spectra were recorded on JEOL Eclipse 400 and Bruker Avance III 400 spectrometers at room temperature. ^{1}H NMR chemical shifts are referenced with respect to the chemical shift of the residual protons present in the deuterated solvents ($CDCl_3$, δ_H = 7.26 ppm, δ_C = 77.16 ppm; [D6]-DMSO, δ_H = 2.50 ppm, δ_C = 39.52 ppm). Explicit structure assignments are based on 2D-NMR- measurements (HMBC, HSQC). UV−vis spectra were recorded on a Varian Cary 50 spectrophotometer and a PerkinElmer Lambda 18 (200−600 nm) in dilute (~10^{-5} M) THF solutions. IR spectra were recorded on a PerkinElmer Spectrum 100 FTIR (ATR) spectrometer. Melting points are not corrected and were measured with a Krüss-Meltingpointmeter KFP I N. High resolution mass spectra were recorded of 1 μM dilute samples in acetonitrile−acetone−water-solutions on a Bruker micrO-TOF II mass spectrometer. Elemental analyses were carried out in the microanalytical laboratory of the University of Konstanz using an Elementar Vario EL CHN analyzer.

X-ray Crystallography. Suitable single crystals of [L^4Ti(dipic)^1] and [L^6Ti(dipic)^1] were grown by slow diffusion of hexane into saturated solutions in dichloromethane. [L^2Ti(dipic)^1] was crystallized from a saturated solution in chloroform by slow evaporation. Crystals were directly picked from solution and covered in an inert oil and immediately placed in the cold N_2-stream of the Oxford Cryostream 700 with nitrogen as coolant gas. Single-crystal X-ray diffraction data collections were performed at 100 K using a STOE IPDS-II diffractometer equipped with a graphite monochromated radiation source (λ = 0.71073 Å) and an image plate detection system. The selection, integration, and averaging procedure of the measured reflex intensities, the determination of the unit cell by a least-squares fit of the 2Θ values, data reduction, LP correction, and the space group determination were performed using the X-Area software package delivered with the diffractometer. A semiempirical absorption correction method was performed after indexing of the crystal faces. The structures of [L^2Ti(dipic)^1] and [L^4Ti(dipic)^1] were solved by direct methods (SHELXS-97),[48] and the structure of [L^6Ti(dipic)^1] was solved by direct methods (SIR97).[49] All structures were refined by standard Fourier techniques against F square with a full-matrix leastsquares algorithm using SHELXL-97or 2013[48] and the WinGX (1.80.05)[50] software package.

All non-hydrogen atoms were refined anisotropically. Hydrogen atoms were placed in calculated positions and refined with a riding model. Graphical representations were prepared with ORTEP-III.[51] Crystallographic data (excluding structure factors) have been deposited with the Cambridge Crystallographic Data Centre as supplementary publication nos. CCDC 995165 [L^2Ti(dipic)^1], CCDC 995166 [L^6Ti(dipic)^1], and CCDC 995167 [L^4Ti(dipic)^1]. Copies of the data can be obtained free of charge on application to CCDC, 12 Union Road, Cambridge CB21EZ, U.K. (Fax: (+44)1223-336-033. E-mail: deposit@ccdc.cam.ac.uk or http://www.ccdc.cam.ac.uk).

Hydrolysis Study. Hydrolysis was studied by observing the time-resolved decrease of the LMCT-band by UV−vis spectroscopy. Equal volumes of dilute samples of the compounds in THF (10^{-5} M) and of buffer solutions of given pH were added to a quartz-cuvette equipped with a magnetic stirring bar. Recording of the spectra was immediately started and repeated in certain time intervals.

pH Measurements. The pH values were determined using a HANNA HI 83141 pH-meter with a HI 1230B pH electrode and a HI 7669AW temperature probe. Calibration was achieved with buffer solutions at pH 4, 7, and 10 (Carl Roth, Karlsruhe). The addition of 50% of THF to the aqueous phosphate-buffer solution influences the autoprotolysis of water and shifts the pH toward more basic values.[52] Direct measurements of the pH in all three THF/buffer mixtures with a pH-meter calibrated with aqueous standards resulted in pH-values of 2.92, 7.52, and 12.21, respectively. However, these pH-values are specific for the chosen solvent system only and are not directly comparable to pH-values determined in pure aqueous media (Table 5).[53] Nevertheless, the above values give a good approximation of the pH-shift caused by the added THF.

Table 5. Compositions of Buffer Solutions per 100 mL Water

	H_3PO_4	KH_2PO_4	K_2HPO_4	K_3PO_4
pH 1.9	2.5 mmol	2.9 mmol		
pH 6.8		3.6 mmol	2.4 mmol	
pH 12.1			2.5 mmol	2.5 mmol

Cytotoxicity Assay. Cytotoxicity was measured on HeLa S3 and Hep G2 cells using an AlamarBlue (Thermo Scientific) assay.[54] Cells were cultivated at 37 °C in humidified 5% CO_2 atmosphere using Dulbecco's DMEM-media (Invitrogen) containing 10% fetal calf serum (Biochrome AG), 1% penicillin, and 1% streptomycin (both GIBCO). Cells were split twice per week. Both cell lines were tested on mycoplasma infections using a mycoplasma detection kit (Roche Applied Science). The cells were seeded in 96-well plates (4.000 HeLa S3 cells/well or 8.000 Hep G2 cells/well) and allowed to attach for 24 h. The cells were then incubated with different concentrations of the reagent to be tested. Complexes were dissolved in a suitable amount of DMSO, and different concentrations were prepared by serial dilution with DMSO. One part of each DMSO solution is then added to 99 parts of medium. Cells were then incubated for 48 h with 100 μL of the above medium containing 1% DMSO and a certain concentration of compound. The medium was then replaced by 100 μL of medium containing 10% AlamarBlue (BioSource Europe), and the cells were incubated for 90 min, The fluorescence at 590 nm was measured after excitation at 530 nm using a Synergy HT Microplate Reader (BioTek). Raw readout data from the assay was corrected for background fluorescence by an "on-plate" blind containing only medium, 1% DMSO, and Alamarblue but no cells (0-value). The background corrected absolute read-outs were then expressed as relative values with regard to an "on-plate" 100% standard containing untreated cells in medium with 1% DMSO. All data was then fitted to a sigmoidal dose−response model with variable slope (4 parameter logistic nonlinear regression model) using Sigma plot 10.0.[55] Upper and lower boundaries as well as the slope were allowed to refine freely. All experiments were repeated at least three times on three different days with each experiment done in four replicates on the same plate. Replicates are treated with equal statistical weight; error-bars represent the SEM. IC_{50} values are given as the means from independent experiments, and the error values of IC_{50} are based on the standard deviation of independent experiments.

Complex Syntheses. ***General Remarks!*** *All handling of air and moisture sensitive compounds has been conducted under an inert atmosphere of dry, oxygen free nitrogen in dry solvents until otherwise noted.*

(2,2′-(Ethane-1,2-diylbis(thiomethylene))bis(4,6-dimethylphenolato))-(pyridine-2,6-dicarboxylato-N,O,O′)-titanium(IV) [L^2Ti(dipic)^1]. Neat titanium tetraisopropoxide (0.78 g, 2.75 mmol) was added to a stirred solution of H_2L^2 (1 g, 2.75 mmol) in anhydrous THF (20 mL). After stirring for 3 h, dipic^1 (0.46 g, 2.75 mmol) was added to the now yellow solution. Stirring was continued for an additional 12 h upon which the red suspension was filtered over a sintered glass-frit and carefully washed with cold THF. [L^2Ti(dipic)^1] was isolated as red crystals (1.4 g, 89%, 2.45 mmol). ^{1}H NMR (400 MHz, $CDCl_3$, ppm): δ = 2.12−2.18 (m, 14H, Ar−CH_3, Ar−CH_3, SC<u>H</u>H′C<u>H</u>H′S), 2.50 (d, ^2J = 8.6 Hz, 2H, SCH<u>H</u>′CH<u>H</u>′S), 3.65 (d, ^2J

DOI: 10.1021/acs.inorgchem.5b00690
Inorg. Chem. 2015, 54, 6697−6706

= 14 Hz, 2H, Ar−CHH′S), 4.45 (d, ^2J = 14 Hz, 2H, Ar−CHH′S), 6.65 (s, 2H, Ar−CH), 6.84 (s, 2H, Ar−CH), 8.29−8.31 (m, 2H, Py-CH), 8.37−8.41 (m, 1H, Py-CH). ^{13}C NMR (101 MHz, $CDCl_3$, ppm): δ = 16.4 (CH_3), 20.8 (CH_3), 34.3 (SCH_2CH_2S), 37.3 (Ar−CH_2S), 124.6 (C-CH_3), 126.5 (Py-CH), 127.6 (C-CH_2S), 127.7 (Ar−CH), 131.40 (C-CH_3), 131.45 (Ar−CH), 144.6 (Py-CH), 149.8 (C═O), 160.9 (C−O), 168.5 (Py-C). UV−vis (THF): λ_{max} (ε) = 270 (21672 $M^{-1}cm^{-1}$), 401 (9146 $M^{-1}cm^{-1}$) nm. IR (ATR): ν = 3080 (w), 2937 (w), 1677 (s), 1473 (m), 1333 (s), 1246 (s), 1173 (s), 1069 (m), 841 (s), 738 (s) cm^{-1}. M.p.: decomp. > 300 °C. Elemental analysis calcd. in %: C 56.55, H 4.75, N 2.44, S 11.18. Found: C 56.42, H 4.74, N 2.50, S 11.15.

(2,2′-(Ethane-1,2-diylbis((methylimino)methylene))bis(4,6-dichlorphenolato))-(pyridine-2,6-dicarboxylato-N,O,O′)-titanium(IV) [L^{3}Ti(dipic)^1]. Dipic^1 (0.21 g, 1.25 mmol) dissolved in *N*,*N*′-dimethylformamide (5 mL) was added to a stirred solution of [$L^3Ti(O^iPr)_2$] (0.5 g, 0.83 mmol) in CH_2Cl_2 (20 mL). The color of the reaction mixture turned dark red within minutes. After 12 h stirring at r.t., the orange colored precipitate was filtered off and washed with small portions of THF. Residual solvent traces were removed by heating to 170 °C for 24 h under reduced pressure (10^{-3} mbar) to yield [L^{3}Ti(dipic)^1] as an orange colored solid (0.46 g, 86%, 0.71 mmol). ^{1}H NMR (400 MHz, $CDCl_3$, ppm): δ = 2.26 (d, ^2J = 9.3 Hz, 2H, NCHH′CHH′N), 2.79 (s, 6H, NCH_3), 3.21 (d, ^2J = 14.6 Hz, 2H, Ar−CHH′N), 3.29 (d, ^2J = 9.3 Hz, 2H, NCHH′CHH′N), 5.34 (d, ^2J = 14.6 Hz, 2H, Ar−CHH′N), 6.91 (d, ^4J = 2.4 Hz, 2H, Ar−CH), 7.16 (d, ^4J = 2.4 Hz, 2H, Ar−CH), 8.19−8.21 (m, 2H, Py-CH), 8.29−8.32 (m, 1H, Py-CH). ^{13}C NMR (101 MHz, $CDCl_3$, ppm): δ = 47.4 (NCH_3), 54.0 (NCH_2CH_2N), 63.6 (Ar−CH_2N), 122.4 (C−Cl), 126.0 (C−Cl), 126.2 (Py-CH), 128.0 (Ar−CH), 129.1 (Ar−CH), 129.9 (C-CH_2N), 144.2 (Py-CH), 149.5 (C═O), 154.0 (C−O), 168.8 (Py-C). UV−vis (THF): λ_{max} (ε) = 265 (19248 $M^{-1}cm^{-1}$), 391 (15551 $M^{-1}cm^{-1}$) nm. IR (ATR): ν = 3052 (w), 2903 (w), 1678 (s), 1457 (s), 1342 (s), 1178 (s), 1068 (m), 877 (s), 777 (s) cm^{-1}. M.p.: decomp. > 337 °C. R_f 0.34 (EE/PE, 1:1). HRMS ([M-H]$^+$, *m*/*z*) calcd.: 649.9714. Found: 649.9703. Elemental analysis calcd. in %: C 46.26, H 3.26, N 6.47. Found: C 46.12, H 3.45, N 6.61.

(2,2′-(Ethane-1,2-diylbis((methylimino)methylene))bis(4,6-di-tert.-butylphenolato))-(pyridine-2,6-dicarboxylato-N,O,O′)-titanium(IV) [L^{4}Ti(dipic)^1]. Neat titanium isopropoxide (0.16 g, 0.57 mmol) was added to a stirred solution of H_2L^4 (0.3 g, 0.57 mmol) in anhydrous THF (30 mL) at r.t. Stirring was continued until NMR-spectroscopy showed the consumption of all starting materials. Dipic^1 (0.15 g, 0.86 mmol) was added at r.t. to this THF-solution of [$L^4Ti(OiPr)_2$]. The reaction progress was followed by NMR-spectroscopy, and after no further isopropanol was liberated, the mixture was evacuated to dryness, taken up in CH_2Cl_2 and purified by flash chromatography. After the removal of the solvent at the rotary evaporator, residual solvent traces were removed by heating to 170 °C for 24 h under reduced pressure (10^{-3} mbar) to yield [L^{4}Ti(dipic)^1] as a red solid (0.38 g, 90%, 0.51 mmol). ^{1}H NMR (400 MHz, $CDCl_3$, ppm): δ = 1.03 (s, 18H, C(CH_3)$_3$), 1.23 (s, 18H, C(CH_3)$_3$), 2.29 (d, ^2J = 9.3 Hz, 2H, NCHH′CHH′N), 2.83 (s, 6H, NCH_3), 3.24 (d, ^2J = 14.2 Hz, 2H, Ar−CHH′N), 3.56 (d, ^2J = 9.3 Hz, 2H, NCHH′CHH′N), 5.26 (d, ^2J = 14.2 Hz, 2H, Ar−CHH′N), 6.84 (d, ^4J = 2.5 Hz, 2H, Ar−CH), 7.08 (d, ^4J = 2.5 Hz, 2H, Ar−CH), 8.14−8.23 (m, 3H, Py-CH). ^{13}C NMR (101 MHz, $CDCl_3$, ppm): δ = 29.7 (C(CH_3)$_3$), 31.7 (C(CH_3)$_3$), 34.5 (C(CH_3)$_3$), 34.8 (C(CH_3)$_3$), 49.0 (NCH_3), 54.8 (NCH_2CH_2N), 65.3 (Ar−CH_2N), 123.5 (Ar−CH), 124.6 (Ar−CH), 125.7 (Py-CH), 127.8 (C-CH_2N), 136.3 (C-^{t}Bu), 143.4 (C-^{t}Bu), 143.6 (Py-CH), 150.2 (C═O), 156.8 (C−O), 169.1 (Py-C). UV−vis (THF): λ_{max} (ε) = 273 (18946 $M^{-1}cm^{-1}$), 406 (13704 $M^{-1}cm^{-1}$) nm. IR (ATR): ν = 2953 (m), 1683 (s), 1466 (m), 1339 (s), 1247 (s), 1171 (s), 915 (m), 850 (s), 760 (s) cm^{-1}. M.p.: > 360 °C. R_f 0.7 (EA:PE/4:1). HRMS ([M-H]$^+$, *m*/*z*) calcd.: 736.3804. Found: 736.3769. Elemental analysis calcd. in %: C 66.93, H 7.81, N 5.71. Found: C 66.69, H 7.93, N 5.82.

(2,2′-(Ethane-1,2-diylbis((methylimino)methylene))bis(6-methoxyphenolato))-(pyridine-2,6-dicarboxylato-N,O,O′)-titanium(IV) [L^{5}Ti(dipic)^1]. This compound was synthesized following the procedure for [L^{3}Ti(dipic)^1]. [$L^5Ti(O^iPr)_2$] (0.3 g, 0.57 mmol) and dipic^1 (0.1 g, 0.57 mmol) were used. After the removal of the solvent, crude [L^{5}Ti(dipic)^1] was purified by column chromatography on silica gel (ethyl acetate). After the removal of the solvent at the rotary evaporator, residual solvent was removed by heating to 170 °C for 24 h under reduced pressure (10^{-3} mbar) to yield [L^{5}Ti(dipic)^1] as a red solid (0.20 g, 62%, 0.35 mmol). ^{1}H NMR (400 MHz, $CDCl_3$, ppm): δ = 2.16 (d, ^2J = 9.3 Hz, 2H, NCHH′CHH′N), 2.78 (s, 6H, NCH_3), 3.21 (d, ^2J = 14.2 Hz, 2H, Ar−CHH′N), 3.38 (d, ^2J = 9.3 Hz, 2H, NCHH′CHH′N), 3.61 (s, 6H, OCH_3), 5.38 (d, ^2J = 14.2 Hz, 2H, Ar−CHH′N), 6.61 (dd, ^3J = 7.1 Hz, ^4J = 1.6 Hz, 2H, Ar−CH) 6.68−6.75 (m, 4H, Ar−CH), 8.15−8.24 (m, 3H, Py-CH). ^{13}C NMR (101 MHz, $CDCl_3$, ppm): δ = 47.5 (NCH_3), 54.0 (NCH_2CH_2N), 56.8 (O−CH_3), 64.1 (Ar−CH_2N), 113.9, 121.5, 122.1 (Ar−CH), 125.9 (Py-CH), 129.3 (C-CH_2N), 143.4 (Py-CH), 147.4 (C-OCH_3), 150.0 (C−O), 150.1 (C═O), 169.1 (Py-C). UV−vis (THF): λ_{max} (ε) = 267 (19713 $M^{-1}cm^{-1}$), 408 (13799 $M^{-1}cm^{-1}$) nm. IR (ATR): ν = 2837 (w), 1676 (s), 1574 (m), 1474 (m), 1342 (s), 1235 (s), 1179 (s), 1002 (m), 876 (s), 742 (s) cm^{-1}. M.p.: decomp. > 300 °C. R_f 0.15 (EE). HRMS ([M-H]$^+$, *m*/*z*) calcd.: 572.1510. Found: 572.1496. Elemental analysis calcd. in %: C 56.75, H 5.12, N 7.35. Found: C 56.71, H 5.16, N 7.32.

(2,2′-(Ethane-1,2-diylbis((methylimino)methylene))bis(5-trifluormethylphenolato))-(pyridine-2,6-dicarboxylato-N,O,O′)-titanium-(IV) [L^{6}Ti(dipic)^1]. This compound was synthesized following the procedure for [L^{4}Ti(dipic)^1]. H_2L^6 (0.3 g, 0.69 mmol), titanium isopropoxide (0.20 g, 0.69 mmol), and dipic^1 (0.18 g, 1.04 mmol) were used. After column chromatography on silica gel (ethyl acetate/petrol ether; 1:1) and removal of solvent residues by heating to 170 °C/10^{-3} mbar for 24 h, [L^{6}Ti(dipic)^1] was isolated as yellow crystals (0.40 g, 88%, 0.62 mmol). ^{1}H NMR (400 MHz, $CDCl_3$, ppm): δ = 2.28 (d, ^2J = 9.4 Hz, 2H, NCHH′CHH′N), 2.82 (s, 6H, NCH_3), 3.31−3.35 (m, 4H, Ar−CHH′N, NCHH′CHH′N), 5.39 (d, ^2J = 14.7 Hz, 2H, Ar−CHH′N), 6.67 (d, ^4J = 1.8 Hz, 2H, Ar−CH), 7.06 (dd, ^3J = 8 Hz, ^4J = 1.8 Hz, 2H, Ar−CH), 7.12 (d, ^3J = 8 Hz, 2H, Ar−CH), 8.20−8.22 (m, 2H, Py-CH), 8.29−8.32 (m, 1H, Py-CH). ^{13}C NMR (101 MHz, $CDCl_3$, ppm): δ = 47.8 (NCH_3), 54.2 (NCH_2CH_2N), 64.0 (Ar−CH_2N), 113.7 (q, $^3J_{CF}$ = 3.7 Hz, Ar−CH), 118.2 (q, $^3J_{CF}$ = 3.8 Hz, Ar−CH), 123.8 (q, $^1J_{CF}$ = 272.4 Hz, CF_3), 126.3 (Py-CH), 130.2 (Ar−CH), 131.3 (C-CH_2N), 131.6 (q, $^2J_{CF}$ = 32.7 Hz, C-CF_3), 144.1 (Py-CH), 149.6 (C═O), 159.4 (C−O), 169.0 (Py-C). ^{19}F NMR (376 MHz, $CDCl_3$, ppm): δ = −62.74 (s, 6F, CF_3). UV−vis (THF): λ_{max} (ε) = 369 (12461 $M^{-1}cm^{-1}$) nm. IR (ATR): ν = 2912 (w), 1693 (s), 1575 (w), 1413 (m), 1324 (s), 1240 (m), 1122 (s), 999 (m), 941 (s), 883 (s), 810 (m), 742 (s) cm^{-1}. M.p.: = 268 °C. R_f 0.18 (EA:PE/1:1). HRMS ([M-H]$^+$, *m*/*z*) calcd.: 648.1046. Found: 648.1027. Elemental analysis calcd. in %: C 50.10, H 3.58, N 6.49. Found: C 49.81, H 3.88, N 6.43.

(2,2′-(Ethane-1,2-diylbis((methylimino)methylene))bis(4,6-dimethylphenolato))-(4-methoxypyridine-2,6-dicarboxylato-N,O,O′)-titanium(IV) [L^{1}Ti(dipic)^2]. This compound was synthesized following the procedure for [L^{4}Ti(dipic)^1]. H_2L^1 (0.2 g, 0.58 mmol), titanium isopropoxide (0.16 g, 0.58 mmol), and dipic^2 (0.11 g, 0.58 mmol) were used. After column chromatography on silica gel (ethyl acetate) and removal of solvent residues by heating to 170 °C/10^{-3} mbar for 24 h, [L^{1}Ti(dipic)^2] was isolated as red crystals (0.20 g, 60%, 0.35 mmol). ^{1}H NMR (400 MHz, $CDCl_3$, ppm): δ = 1.92 (s, 6H, Ar−CH_3), 2.10 (d, ^2J = 9.3 Hz, 2H, NCHH′CHH′N), 2.18 (s, 6H, Ar−CH_3), 2.74 (s, 6H, NCH_3), 3.12 (d, ^2J = 14.2 Hz, 2H, Ar−CHH′N), 3.35 (d, ^2J = 9.3 Hz, 2H, NCHH′CHH′N), 4.02 (s, 3H, O−CH_3), 5.25 (d, ^2J = 14.2 Hz, 2H, Ar−CHH′N), 6.63 (d, ^4J = 1.8 Hz, 2H, Ar−CH), 6.75 (d, ^4J = 1.8 Hz, 2H, Ar−CH), 7.58 (s, 2H, Py-CH). ^{13}C NMR (101 MHz, $CDCl_3$, ppm): δ = 16.1 (Ar−CH_3), 20.8 (Ar−CH_3), 47.1 (NCH_3), 53.9 (NCH_2CH_2N), 57.2 (O−CH_3), 64.0 (Ar−CH_2N), 111.0 (Py-CH), 125.1 (C-CH_3), 127.5 (C-CH_2N), 127.8 (Ar−CH), 130.5 (C-CH_3), 130.7 (Ar−CH), 152.1 (C═O), 156.2 (C−O), 169.1 (Py-C), 171.4 (C-OCH_3). UV−vis (THF): λ_{max} (ε) = 268 (20722 $M^{-1}cm^{-1}$), 398 (13335 $M^{-1}cm^{-1}$) nm. IR (ATR): ν = 2912 (w), 1678 (s), 1617 (m), 1470 (m), 1364 (s), 1245 (s), 1053 (s), 850 (s), 748 (m) cm^{-1}. M.p.: decomp. > 360 °C. R_f 0.38 (EE). HRMS ([M-H]$^+$,

DOI: 10.1021/acs.inorgchem.5b00690
Inorg. Chem. 2015, 54, 6697−6706

m/*z*) calcd.: 598.2030. Found: 598.2008. Elemental analysis calcd. in %: C 60.31, H 5.90, N 7.03. Found: C 60.31, H 6.07, N 7.12.

(2,2′-(Ethane-1,2-diylbis((methylimino)methylene))bis(4,6-dimethylphenolato))-(4-hydroxymethylpyridine-2,6-dicarboxylato-N,O,O′)-titanium(IV) [L¹Ti(dipic)³]. This compound was synthesized following the procedure for [L³Ti(dipic)¹]. [L¹Ti(O^{iPr})$_2$] (0.3 g, 0.58 mmol) and dipic³ (0.11 g, 0.87 mmol) were used. After removal of the solvent, the crude product was washed several times with small amounts of THF and sonicated for 15 min in pentane. After filtration, the bright orange precipitate was dried at 170 °C for 24 h under reduced pressure (10^{-3} mbar) to yield [L¹Ti(dipic)³] as a bright orange solid (0.25 g, 73%, 0.42 mmol). ^{1}H NMR (400 MHz, $CDCl_3$, ppm): δ = 1.86 (s, 6H, Ar−CH_3), 2.10 (d, ^2J = 9.3 Hz, 2H, NCHH′CHH′N), 2.16 (s, 6H, Ar−CH_3), 2.74 (s, 6H, NCH_3), 3.13 (d, ^2J = 14.2 Hz, 2H, Ar−CHH′N), 3.34 (d, ^2J = 9.3 Hz, 2H, NCHH′CHH′N), 4.96 (s, 2H, Py-CH_2−OH), 5.25 (d, ^2J = 14.2 Hz, 2H, Ar−CHH′N), 6.63 (s, 2H, Ar−CH), 6.71 (s, 2H, Ar−CH), 8.22 (s, 2H, Py-CH). ^{13}C NMR (101 MHz, $CDCl_3$, ppm): δ = 16.0 (Ar−CH_3), 20.8 (Ar−CH_3), 47.2 (NCH_3), 54.0 (N$CH_2$$CH_2$N), 63.2 (Ar−$CH_2$N), 64.1 (Py-$CH_2$−OH), 122.8 (Py-CH), 125.1 (C-CH_3), 127.5 (C-CH_2N), 127.9 (Ar−CH), 130.66 (C-CH_3), 130.74 (Ar−CH), 150.0 (C═O), 156.1 (C−O), 160.0 (C-CH_2−OH), 169.4 (Py-C). UV−vis (THF): λ_{max} (ε) = 270 (14862 $M^{-1}cm^{-1}$), 400 (11352 $M^{-1}cm^{-1}$) nm. IR (ATR): ν = 3550 (w), 3301 (w), 2911 (w), 1694 (m), 1662 (s), 1367 (m), 1240 (s), 1164 (m), 850.22 (s), 749.19 (m) cm^{-1}. M.p.: decomp. > 290 °C. HRMS ([M-H]$^+$, *m*/*z*) calcd.: 598.2030. Found: 598.2022. Elemental analysis calcd. in %: C 60.31, H 5.90, N 7.03. Found: C 60.36, H 5.86, N 6.98.

■ ASSOCIATED CONTENT

Supporting Information

Colored representations of the IC_{50} graphs, time-resolved UV−vis spectra of hydrolysis experiments, ^{1}H, ^{13}C, and ^{19}F NMR spectra as well as X-ray diffraction data of [L²Ti(dipic)¹], [L⁴Ti(dipic)¹], and [L⁶Ti(dipic)¹]. The Supporting Information is available free of charge on the ACS Publications website at DOI: 10.1021/acs.inorgchem.5b00690.

■ AUTHOR INFORMATION

Corresponding Author

*Tel: +49-7531-882283. Fax: +49-7531-884424. E-mail: thomas.huhn@uni-konstanz.de.

Present Addresses

†M.G.: MEET Battery Research Center, University of Münster, Corrensstr. 46, D-48149 Münster, Germany.

‡T.A.I.: Lanxess Deutschland GmbH, Chempark Dormagen, D-41538 Dormagen, Germany.

Notes

The authors declare no competing financial interest.

■ ACKNOWLEDGMENTS

We acknowledge Malin Bein for help with the biological experiments and Bernhard Weibert for help with X-ray data analysis. T.Z. and T.A.I. are grateful for personal scholarships of the Konstanz Research School Chemical Biology (KoRS-CB).

■ REFERENCES

(1) Adão, P.; Barroso, S.; Avecilla, F.; Oliveira, M. C.; Pessoa, J. C. *J. Organomet. Chem.* **2014**, *760*, 212−223.

(2) Voronova, K.; Purgel, M.; Udvardy, A.; Bényei, A. C.; Kathó, Á.; Joó, F. *Organometallics* **2013**, *32*, 4391−4401.

(3) Tshuva, E. Y.; Goldberg, I.; Kol, M.; Goldschmidt, Z. *Inorg. Chem.* **2001**, *40*, 4263−4270.

(4) Hormnirun, P.; Marshall, E. L.; Gibson, V. C.; White, A. J. P.; Williams, D. J. *J. Am. Chem. Soc.* **2004**, *126*, 2688−2689.

(5) Tshuva, E. Y.; Goldberg, I.; Kol, M.; Weitman, H.; Goldschmidt, Z. *Chem. Commun.* **2000**, 379−380.

(6) Białek, M.; Pochwała, M.; Spaleniak, G. *J. Polym. Sci., Part A: Polym. Chem.* **2014**, *52*, 2111−2123.

(7) Talsi, E. P.; Bryliakov, K. P. *Appl. Organomet. Chem.* **2013**, *27*, 239−244.

(8) Egami, H.; Matsumoto, K.; Oguma, T.; Kunisu, T.; Katsuki, T. *J. Am. Chem. Soc.* **2010**, *132*, 13633−13635.

(9) Matsumoto, K.; Egami, H.; Oguma, T.; Katsuki, T. *Chem. Commun.* **2012**, *48*, 5823−5825.

(10) Shavit, M.; Peri, D.; Manna, C. M.; Alexander, J. S.; Tshuva, E. Y. *J. Am. Chem. Soc.* **2007**, *129*, 12098−12099.

(11) Immel, T. A.; Debiak, M.; Groth, U.; Bürkle, A.; Huhn, T. *ChemMedChem* **2009**, *4*, 738−741.

(12) Tshuva, E. Y.; Peri, D. *Coord. Chem. Rev.* **2009**, *253*, 2098−2115.

(13) Immel, T. A.; Groth, U.; Huhn, T.; Öhlschlager, P. *PLoS One* **2011**, *6*, e17869.

(14) Manna, C. M.; Braitbard, O.; Weiss, E.; Hochman, J.; Tshuva, E. Y. *ChemMedChem* **2012**, *7*, 703−708.

(15) Immel, T. A.; Groth, U.; Huhn, T. *Chem. - Eur. J.* **2010**, *16*, 2775−2789.

(16) Peri, D.; Meker, S.; Manna, C. M.; Tshuva, E. Y. *Inorg. Chem.* **2011**, *50*, 1030−1038.

(17) Meker, S.; Margulis-Goshen, K.; Weiss, E.; Magdassi, S.; Tshuva, E. Y. *Angew. Chem., Int. Ed.* **2012**, *51*, 10515−10517.

(18) Miller, M.; Tshuva, E. Y. *Eur. J. Inorg. Chem.* **2014**, *2014*, 1485−1491.

(19) Reytman, L.; Braitbard, O.; Tshuva, E. Y. *Dalton Trans.* **2012**, *41*, 5241−5247.

(20) Matos, C. P.; Valente, A.; Marques, F.; Adão, P.; Paula Robalo, M.; de Almeida, R. F. M.; Pessoa, J. C.; Santos, I.; Helena Garcia, M.; Tomaz, A. I. *Inorg. Chim. Acta* **2013**, *394*, 616−626.

(21) Jeslin Kanaga Inba, P.; Annaraj, B.; Thalamuthu, S.; Neelakantan, M. A. *Bioinorg. Chem. Appl.* **2013**, *2013*, 1.

(22) Peri, D.; Meker, S.; Shavit, M.; Tshuva, E. Y. *Chem. - Eur. J.* **2009**, *15*, 2403−2415.

(23) Hancock, S. L.; Gati, R.; Mahon, M. F.; Tshuva, E. Y.; Jones, M. D. *Dalton Trans.* **2014**, *43*, 1380−1385.

(24) Schwarzenbach, G. *Helv. Chim. Acta* **1952**, *35*, 2344−2359.

(25) Munro, D. *Chem. Br.* **1977**, *13*, 100−105.

(26) Immel, T. A.; Grützke, M.; Späte, A.-K.; Groth, U.; Öhlschläger, P.; Huhn, T. *Chem. Commun.* **2012**, *48*, 5790−5792.

(27) Walsh, P. J.; Balsells, J.; Carroll, P. J. *Inorg. Chem.* **2001**, *40*, 5568−5574.

(28) Immel, T. A.; Grützke, M.; Batroff, E.; Groth, U.; Huhn, T. *J. Inorg. Biochem.* **2012**, *106*, 68−75.

(29) Tshuva, E. Y.; Gendeziuk, N.; Kol, M. *Tetrahedron Lett.* **2001**, *42*, 6405−6407.

(30) Fries, K.; Brandes, E. *Justus Liebigs Ann. Chem.* **1939**, *542*, 48−77.

(31) Cohen, A.; Yeori, A.; Goldberg, I.; Kol, M. *Inorg. Chem.* **2007**, *46*, 8114−8116.

(32) Bradshaw, J. S.; Maas, G. E.; Lamb, J. D.; Izatt, R. M.; Christensen, J. J. *J. Am. Chem. Soc.* **1980**, *102*, 467−474.

(33) Shelkov, R.; Melman, A. *Eur. J. Org. Chem.* **2005**, *2005*, 1397−1401.

(34) Tang, R.; Zhao, Q.; Yan, Z.; Luo, Y. *Synth. Commun.* **2006**, *36*, 2027−2034.

(35) Quiroz-Guzman, M.; Oliver, A. G.; Loza, A. J.; Brown, S. N. *Dalton Trans.* **2011**, *40*, 11458−11468.

(36) Nakata, N.; Toda, T.; Matsuo, T.; Ishii, A. *Inorg. Chem.* **2012**, *51*, 274−281.

(37) Ishii, A.; Asajima, K.; Toda, T.; Nakata, N. *Organometallics* **2011**, *30*, 2947−2956.

(38) Cohen, A.; Goldberg, I.; Venditto, V.; Kol, M. *Eur. J. Inorg. Chem.* **2011**, *2011*, 5219−5223.

(39) Buettner, K. M.; Valentine, A. M. *Chem. Rev.* **2012**, *112*, 1863−1881.

DOI: 10.1021/acs.inorgchem.5b00690
Inorg. Chem. 2015, 54, 6697−6706

(40) Barroso, S.; Coelho, A. M.; Gomez-Ruiz, S.; Calhorda, M. J.; Zizak, Z.; Kaluderovic, G. N.; Martins, A. M. *Dalton Trans.* **2014**, *43*, 17422−17433.
(41) Pearson, R. G. *J. Am. Chem. Soc.* **1963**, *85*, 3533−3539.
(42) Cordero, B.; Gomez, V.; Platero-Prats, A. E.; Reves, M.; Echeverria, J.; Cremades, E.; Barragan, F.; Alvarez, S. *Dalton Trans.* **2008**, 2832−2838.
(43) Immel, T. A. Ph.D. Thesis. Universität Konstanz, Konstanz, Germany, 2011.
(44) Schur, J.; Manna, C. M.; Tshuva, E. Y.; Ott, I. *Metallodrugs* **2014**, *1*, 1−9.
(45) Schur, J.; Manna, C. M.; Deally, A.; Koster, R. W.; Tacke, M.; Tshuva, E. Y.; Ott, I. *Chem. Commun.* **2013**, *49*, 4785−4787.
(46) Using 6 mg of complex with an average molecular weight of 600 g/mol in the NMR sample of approximately 0.5 mL NMR solvent renders the sample 20 mmol/L. Then adding 1000 equiv. of D_2O amounts to 400 g/L or 200 μL per NMR sample giving a total volume of 0.70 mL in the NMR tube.
(47) Armarego, W. L. F.; Chai, C. L. L. Purification of Laboratory Chemicals, 5th ed.; Elsevier Science/Butterworth Heinemann: Amsterdam, 2003.
(48) Sheldrick, G. *Acta Crystallogr., Sect. A: Found. Crystallogr.* **2008**, *64*, 112−122.
(49) Cascarano, G.; Altomare, A.; Giacovazzo, C.; Guagliardi, A.; Moliterni, A. G. G.; Siliqi, D.; Burla, M. C.; Polidori, G.; Camalli, M. *Acta Crystallogr., Sect. A: Found. Crystallogr.* **1996**, *52*, C79.
(50) Farrugia, L. *J. Appl. Crystallogr.* **1999**, *32*, 837−838.
(51) Farrugia, L. *J. Appl. Crystallogr.* **1997**, *30*, 565.
(52) Barbosa, J.; Barrón, D.; Butí, S. *Anal. Chim. Acta* **1999**, *389*, 31−42.
(53) Rondinini, S.; Nese, A. *Electrochim. Acta* **1987**, *32*, 1499−1505.
(54) Fields, R. D.; Lancaster, M. V. *Am. Biotechnol. Lab.* **1993**, *11*, 48−49.
(55) Systat Software, Inc. 2006. http://www.systat.com.

DOI: 10.1021/acs.inorgchem.5b00690
Inorg. Chem. 2015, 54, 6697−6706